

Reliable Eigenspectra for New Generation Surveys

Tamás Budavári^{1*}, Vivienne Wild², Alexander S. Szalay^{1,2}, László Dobos³, and Ching-Wa Yip¹

¹*Department of Physics and Astronomy, The Johns Hopkins University, 3701 San Martin Drive, Baltimore, MD 21218, USA*

²*Max Planck Institute for Astrophysics, Karl-Schwarzschild Str. 1, 85741 Garching, Germany*

³*Eötvös Loránd University, Department of Physics of Complex Systems, Pázmány P. sétány 1/A, Budapest, 1117, Hungary*

21 June 2024

ABSTRACT

We present a novel technique to overcome the limitations of the applicability of Principal Component Analysis to typical real-life data sets, especially astronomical spectra. Our new approach addresses the issues of outliers, missing information, large number of dimensions and the vast amount of data by combining elements of robust statistics and recursive algorithms that provide improved eigensystem estimates step-by-step. We develop a generic mechanism for deriving reliable eigenspectra without manual data censoring, while utilising all the information contained in the observations. We demonstrate the power of the methodology on the attractive collection of the VIMOS VLT Deep Survey spectra that manifest most of the challenges today, and highlight the improvements over previous workarounds, as well as the scalability of our approach to collections with sizes of the Sloan Digital Sky Survey and beyond.

Key words: galaxies: statistics — methods: statistical

1 MOTIVATION

As modern telescopes collect more and more data in our exponential world, where the size of the detectors essentially follows Moore’s law, the kind of statistical challenges astronomers face in analysing the observations change dramatically in nature. We need algorithms that scale well in time and complexity with the volume of the data, while obeying the constraints of today’s computers. But the large data volume is only one of the consequences of this trend. With more observations in hand, the number of problematic detections also increases. In addition to the elegant mathematical theorems that work miracles on textbook examples, scientists need to develop methodologies that provide reliable results that are robust in the statistical sense when applied to real-life data.

One particular multi-variate analysis technique, which is widely accepted and popular not only in astronomy but also in genetics, imaging and many other fields, is Principal Component Analysis (PCA). For its simple geometric meaning and straightforward implementation via Singular Value Decomposition (SVD), it has been utilised in many areas of the field including classification of galaxies and quasars (Francis et al. 1992; Connolly et al. 1995; Connolly & Szalay 1999; Yip et al. 2004a,b), spectroscopic and photometric redshift estimation (Glazebrook, Offer, & Deeley 1998; Budavári et al. 1999, 2000), sky subtraction (Wild & Hewett 2005), and highly efficient optical spectral indicators (Wild et al. 2007). However, direct application of the classic PCA to real data

is almost always impossible; the reasons are usually three-fold: (1) The technique is extremely sensitive to outliers. With smaller datasets, scientists would “clean up” the sample by completely removing the “obvious” outliers in one or more projections and analyse the remaining subset. The problem with this approach is that it is subjective, and it becomes impractical for large datasets. (2) Another problem is missing measurements in the data vectors, e.g., pixels of a spectrum. There are various reasons for this to occur: strong night sky lines, cosmic rays or simply because of the redshift that yields different restframe wavelength coverage for the spectra. The application of PCA implies the assumption of a Euclidean metric, but it is not clear how to calculate Euclidean distances when data is missing from our observed vectors. (3) Last but not least, the memory requirement of SVD is significant as the entire dataset is stored in memory while the decomposition is computed. For example, the Sloan Digital Sky Survey (SDSS) Data Release 6 contains a million spectra with 4000 resolution elements each. While machines certainly exist today that have the required amount of RAM (~ 50 GB), typical workstations have lesser resources. Additionally, in most situations, we only seek a small number of eigenvectors associated with the largest eigenvalues, and SVD computes all the singular vectors in vain.

The optical spectra of the VIMOS VLT Deep Survey (VVDS; Le Fèvre et al. 2005) provides an extremely attractive dataset for galaxy evolution studies at high redshift, yet, due to their generally low signal-to-noise ratio they are unsuitable for traditional PCA. In this case, the challenge does not lie in the volume of the data set, rather in the natural limitations of high redshift observations.

* budavari@jhu.edu

Thanks to the careful processing by the VVDS Team, the spectra are well calibrated and each one contains valuable information for a PCA analysis.

Our goal is to develop an algorithm to address all of the above issues in a way that is true to the spirit of the PCA and maintains its geometrically meaningful properties. In §2 we detail the various layers of our solution to the problem, and in §3 we compare the performance of different techniques when applied to the VVDS spectra. In §4 we evaluate the results of the methods and analyse the emerging physical features. §5 concludes our study.

2 STREAMING PCA

Our approach to the analysis is not the classical one. Instead of working with a *data set*, we aim to formulate the problem using the concept of a *data stream*. We want to incrementally improve our understanding of the properties of the data, deriving better and better eigenspectra through the incremental addition of new observations.

We develop an algorithm to recursively calculate the quantities of interest. As the first step and an illustration of the concept, we look at the calculation of the sample mean,

$$\boldsymbol{\mu} = \frac{1}{N} \sum_{n=1}^N \mathbf{x}_n \quad (1)$$

where $\{\mathbf{x}_n\}$ are the N observation vectors. One can define a series of estimates as

$$\boldsymbol{\mu}_n = \frac{n-1}{n} \boldsymbol{\mu}_{n-1} + \frac{1}{n} \mathbf{x}_n \quad (2)$$

It is easy to see that $\boldsymbol{\mu}_1 = \mathbf{x}_1$ and $\boldsymbol{\mu}_N = \boldsymbol{\mu}$. This iterative formula is the key to our new procedure, where the best estimate of the sample mean at each step is

$$\boldsymbol{\mu} = \gamma \boldsymbol{\mu}_{\text{prev}} + (1 - \gamma) \mathbf{x} \quad (3)$$

$$= \boldsymbol{\mu}_{\text{prev}} + (1 - \gamma) \mathbf{y} \quad (4)$$

where we introduced the centered variable $\mathbf{y} = \mathbf{x} - \boldsymbol{\mu}_{\text{prev}}$. The weight parameter γ lies between 0 and 1, and may be a function of both the observation vector and the iteration step.

2.1 Updating the Eigensystem

The calculation of the sample covariance matrix is essentially identical to that of the mean, except we average the outer products of the vectors. Let us solve for the eigenspectra that belong to the largest p eigenvalues that account for most of the sample variance. This means that the $\mathbf{E}_p \boldsymbol{\Lambda}_p \mathbf{E}_p^T$ is a good approximation to the full covariance matrix, where $\{\boldsymbol{\Lambda}_p, \mathbf{E}_p\}$ is the truncated eigensystem. Hence, the recursion takes the form of

$$\mathbf{C} = \gamma \mathbf{C}_{\text{prev}} + (1 - \gamma) \mathbf{y} \mathbf{y}^T \quad (5)$$

$$\approx \gamma \mathbf{E}_p \boldsymbol{\Lambda}_p \mathbf{E}_p^T + (1 - \gamma) \mathbf{y} \mathbf{y}^T \quad (6)$$

Following Li et al. (2003), we write the covariance matrix as the product of some matrix \mathbf{A} and its transpose

$$\mathbf{C} \approx \mathbf{A} \mathbf{A}^T \quad (7)$$

where the matrix \mathbf{A} has only $(p + 1)$ columns, and is thus much smaller than the covariance matrix. The columns of \mathbf{A} are the constructed from the previous eigenvalues λ_k and eigenspectra \mathbf{e}_k , as

well as the new observation vector \mathbf{y} ,

$$\mathbf{a}_k = \mathbf{e}_k \sqrt{\gamma \lambda_k}, \quad k = 1 \dots p \quad (8)$$

$$\mathbf{a}_{p+1} = \mathbf{y} \sqrt{1 - \gamma} \quad (9)$$

If $\mathbf{A} = \mathbf{U} \mathbf{W} \mathbf{V}^T$ then the eigensystem of the covariance \mathbf{C} will have eigenvalues of $\boldsymbol{\Lambda} = \mathbf{W}^2$ and eigenspectra equal to the singular-vectors, $\mathbf{E} = \mathbf{U}$. Therefore, this formalism allows us to update the eigensystem by solving the SVD of the much smaller \mathbf{A} leading to a significant decrease in computational time.

Following the above procedure, one can update the truncated eigensystem step-by-step by adding the observed spectra one-by-one to build the final basis. A natural starting point for the iteration is to run SVD on a small subset of observation vectors first and proceed with the above updates from there.

2.2 Robustness against Outliers

Before we turn to making the algorithm robust, to understand the limitations of PCA let us first review the geometric problem that PCA solves. The classic procedure essentially fits a hyperplane to the data, where the eigenspectra define the projection matrix onto this plane. If the truncated eigensystem consists of p eigenspectra in the matrix \mathbf{E}_p , the projector is $\mathbf{E}_p \mathbf{E}_p^T$, and the residual of the fit for the n th observation vector is written as

$$\mathbf{r}_n = (\mathbf{I} - \mathbf{E}_p \mathbf{E}_p^T) \mathbf{y}_n \quad (10)$$

Using this notation, PCA simply solves the minimization problem

$$\min \frac{1}{N} \sum_{n=1}^N r_n^2 \quad (11)$$

where $r_n \equiv |\mathbf{r}_n|$. The sensitivity of PCA to outliers comes from the fact that the sum will be dominated by the extreme values in the data set.

Over the last couple of decades, a number of improvements have been proposed to overcome this issue within the framework of robust statistics (e.g., see Maronna, Martin & Yohai 2006, for a concise overview). The current state-of-the-art technique introduced by Maronna (2005) is based on a robust M-estimate (Huber 1981) of the scale, called M-scale. Here we solve the new minimization problem

$$\min \sigma^2 \quad (12)$$

where σ^2 is an M-scale of the residuals r_n^2 , which satisfies the equation

$$\frac{1}{N} \sum_{n=1}^N \rho \left(\frac{r_n^2}{\sigma^2} \right) = \delta \quad (13)$$

where ρ is the robust function. Usually a robust ρ -function is bound and assumed to be scaled to values between $\rho(0) = 0$ and $\rho(\infty) = 1$. The parameter δ controls the breakdown point where the estimate explodes due to too much outlier contamination. It is straightforward to verify that in the non-robust maximum likelihood estimation (MLE) case with $\rho(t) = t$ and $\delta = 1$, we recover the classic minimization problem with σ being the root mean square (RMS).

By implicit differentiation the robust solution yields a very intuitive result: the mean is a weighted average of the observation vectors, and the hyperplane is derived from the eigensystem of a weighted covariance matrix,

$$\boldsymbol{\mu} = \left(\sum w_n \mathbf{x}_n \right) / \left(\sum w_n \right) \quad (14)$$

$$\mathbf{C} = \sigma^2 \left(\sum w_n (\mathbf{x}_n - \boldsymbol{\mu})(\mathbf{x}_n - \boldsymbol{\mu})^T \right) / \left(\sum w_n r_n^2 \right) \quad (15)$$

where $w_n = W(r_n^2/\sigma^2)$ and $W(t) = \rho'(t)$. The weight for each observation vector depends on σ^2 , which suggests the appropriateness of an iterative solution, where in every step we solve for the eigenspectra and use them to calculate a new σ^2 scale; see Maronna (2005) for details. One way to obtain the solution of eq.(13) is to re-write it in the intuitive form of

$$\sigma^2 = \frac{1}{N\delta} \sum_{n=1}^N w_n^* r_n^2 \quad (16)$$

where the weights are $w_n^* = W^*(r_n^2/\sigma^2)$ with $W^*(t) = \rho(t)/t$. Although, this is not the solution as the right hand side contains σ^2 itself, it can be shown that its iterative re-evaluation converges to the solution.

We take this approach one step further. By recursively calculating the eigenspectra instead of the classic method, we can allow for a simultaneous solution for the scale σ^2 , as well. The recursion equation for the mean is formally almost identical to the classic case, and we introduce new equations to propagate the weighted covariance matrix and the scale,

$$\boldsymbol{\mu} = \gamma_1 \boldsymbol{\mu}_{\text{prev}} + (1 - \gamma_1) \mathbf{x} \quad (17)$$

$$\mathbf{C} = \gamma_2 \mathbf{C}_{\text{prev}} + (1 - \gamma_2) \sigma^2 \mathbf{y} \mathbf{y}^T / r^2 \quad (18)$$

$$\sigma^2 = \gamma_3 \sigma_{\text{prev}}^2 + (1 - \gamma_3) w^* r^2 / \delta \quad (19)$$

where the γ coefficients depend on the running sums of 1, w and $w r^2$ denoted below by u , v and q , respectively.

$$\gamma_1 = \alpha v_{\text{prev}} / v \quad \text{with} \quad v = \alpha v_{\text{prev}} + w \quad (20)$$

$$\gamma_2 = \alpha q_{\text{prev}} / q \quad \text{with} \quad q = \alpha q_{\text{prev}} + w r^2 \quad (21)$$

$$\gamma_3 = \alpha u_{\text{prev}} / u \quad \text{with} \quad u = \alpha u_{\text{prev}} + 1 \quad (22)$$

The parameter α introduced here, which takes values between 0 and 1, adjusts the rate at which the evolving solution of the eigenproblem *forgets* about past observations. It sets the characteristic width of the sliding window over the stream of data; in other words, the effective sample size.¹ The value $\alpha = 1$ corresponds to the classic case of infinite memory. Since our iteration starts from a non-robust set of eigenspectra, a procedure with $\alpha < 1$ is able to eliminate the effect of the initial transients. Due to the finite memory of the recursion, it is clearly disadvantageous to put the spectra on the stream in a systematic order; instead they should be randomized for best results.

It is worth noting that robust “eigenvalues” can be computed for any eigenspectra in a consistent way, which enables a meaningful comparison of the performance of various bases. To derive a robust measure of the scatter of the data along a given eigenspectrum e , one can project the data on it, and formally solve the same equation as in eq.(13) but with the residuals replaced with the projected values, i.e., for the k th eigenspectrum $r_n = e_k \mathbf{y}_n$. The resulting σ^2 value is a robust estimate of λ_k .

2.3 Missing Entries in Observations

The other common challenge is the presence of gaps in the observations, i.e., missing entries in the data vectors. Gaps emerge for numerous reasons in real-life measurements. Some cause the loss of random snippets while others correlate with physical properties

of the sources. An example of the latter is the wavelength coverage of objects at different redshifts: the observed wavelength range being fixed, the detector looks at different parts of the electromagnetic spectrum for different extragalactic objects.

Now we face two separate problems. Using PCA implies that we believe the Euclidean metric to be a sensible choice for our data, i.e., it is a good measure of similarity. Often one needs to normalize the observations so that this assumption would hold. For example, if one spectrum is identical to another but the source is brighter and/or closer, their distance would be large. The normalisation guarantees that they are close in the Euclidean metric. So firstly, we must normalise every spectrum before it is entered into the streaming algorithm. This step is difficult to do in the presence of incomplete data, hence we also have to “patch” the missing data.

Inspired by Everson & Sirovich (1995), Connolly & Szalay (1999) proposed a solution, where the gaps are filled by an unbiased reconstruction using a pre-calculated eigenbasis. A final eigenbasis may be calculated iteratively by continuously filling the gaps with the previous eigenbasis until convergence is reached (Yip et al. 2004a). While Connolly & Szalay (1999) allowed for a bias in rotation only, the method has recently been extended to accommodate a shift in the normalisation of the data vectors (Wild et al. 2007, Lemson et al., in preparation). Of course, the new algorithm presented in this paper can use the previous eigenbasis to fill gaps in each input data vector as they are input, thus avoiding the need for multiple iterations through the entire dataset.

The other problem is a consequence of the above solution. Having patched the incomplete data by the current best understanding of the manifold, we have artificially removed the residuals in the bins of the missing entries, thus decreased the length of the residual vector. This would result in increasingly large weights being assigned to spectra with the largest number of empty pixels. One solution is to calculate the residual vector using higher-order eigenspectra. The idea is to solve for not only the first p eigenspectra but a larger $(p+q)$ number of components and estimate the residuals in the missing bins using the difference of the reconstructions on the two different truncated bases.

3 THE VVDS SPECTRA

The VIMOS VLT Deep survey (VVDS) is a deep spectroscopic redshift survey, targetting objects with apparent magnitudes in the range of $17.5 \leq I_{AB} \leq 24$ (Le Fèvre et al. 2005). The survey is unique for high redshift galaxy surveys in having applied no further colour cuts to minimise contamination from stars, yielding a particularly simple selection function, making it a very attractive dataset for statistical studies of the high redshift galaxy population. In this work we make use of the spectra from the publicly available first epoch data release of the VVDS-0226-04 (VVDS-02h) field (Le Fèvre et al. 2005). The spectra have a resolution of $R = 227$ and a dispersion of 7.14 \AA/pixel . They have a usable observed frame wavelength range, for our purposes, of $\sim 5500\text{-}8500 \text{ \AA}$.

The first epoch public data release contains 8981 spectroscopically observed objects in the VVDS-02h field, we select only those with moderate to secure redshifts (flags 2, 3, 4, and 9) that lie in the redshift range $0.5 < z < 1.0$. The redshift range is determined by the rest-frame spectral range we have chosen for this study. The final sample contains 3485 spectra.

The VVDS dataset provides the ideal test for a robust PCA algorithm, because of the low signal-to-noise ratio of the spectra and the significant chance that outliers exist due to incorrect redshift

¹ For example, the sequence u rapidly converges to $1/(1 - \alpha)$.

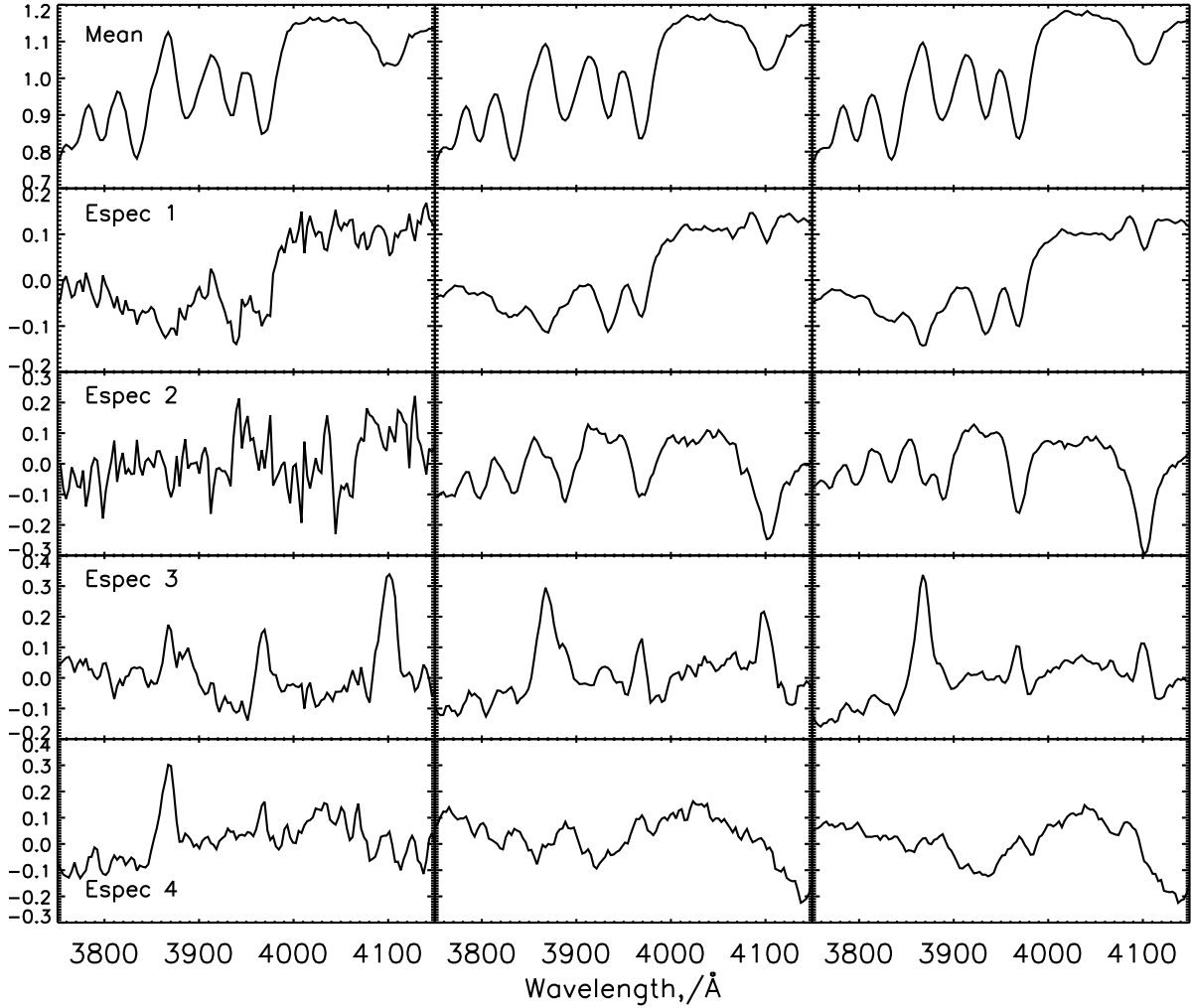


Figure 1. The mean spectrum and top four eigenspectra for the VVDS galaxies. The eigenspectra have been inverted where necessary to make the physical features easier to identify (i.e. absorption lines in absorption and emission lines in emission) *Left:* The result from classic PCA on 3485 spectra. *Center:* The result from classic PCA with iterative removal of outliers. The final dataset contains 2675 spectra. *Right:* The result from the new iterative-robust PCA algorithm.

determinations. We have chosen the 4000\AA break region to illustrate the procedure because of the obvious importance of this spectral region for galaxy evolution studies (e.g., Balogh et al. 1999; Wild et al. 2007) and also due to the wide variety of spectral features present for the PCA to identify. Eigenspectra similar to those created in this analysis will be used by Wild et al. (in preparation) for the identification of $H\delta$ -strong galaxies in the VVDS survey.

3.1 Classic and Trimmed Analysis

To provide a comparison for the robust algorithm, we first perform the classic PCA using an SVD algorithm. The spectra are corrected for Galactic extinction assuming a uniform $E(B-V) = 0.027$ (McCracken et al. 2003), moved to the galaxy rest-frame and interpolated onto a common wavelength grid. Regions of the spectra with bad pixels are identified using the associated error arrays, regions with strong night sky lines are included into the mask. Each spectrum is normalised, by dividing by the median flux in the good pixels, and gaps in the dataset caused by bad pixels are filled with

the median of all other spectra at that wavelength. The mean spectrum is calculated and subtracted, and PCA is then performed on the residuals. The resulting mean spectrum and eigenspectra are presented in the first column of Figure 1.

Clearly the noise level of the eigenspectra resulting from the classic PCA is high. The distribution of principal component amplitudes reveals that the signal in many of the eigenspectra is dominated by a small number of outliers. A natural way to improve on this situation is through the iterative removal of these outliers based on the principal component amplitude distributions. This procedure is essentially the same as the calculation of truncated statistics, e.g., the trimmed mean, when one excludes some percentage of the objects symmetrically based on their rank. For the dataset in question, 20 iterations are required to reduce the number of 3σ outliers in the top 10 eigenspectra to half a dozen, resulting in a total number of 2675 spectra for the final PCA. For a more thorough analysis, a convergence criteria can be employed to indicate when the eigenspectra cease to vary significantly (e.g., Yip et al. 2004a).

The resulting mean and eigenspectra from this trimmed PCA

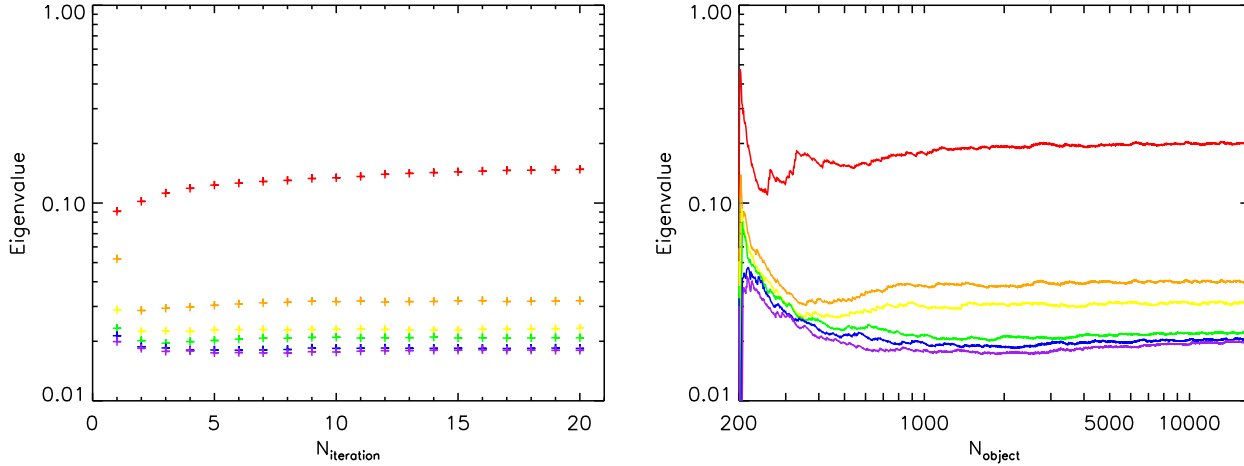


Figure 2. *Left:* The top six normalized eigenvalues as a function of iteration number using the classic PCA. Each eigenvalue represents the amount of sample variance carried by the eigenspectrum. *Right:* The top six normalized eigenvalues as a function of galaxy number for robust streaming PCA. The x-axis begins at 200, the size of the dataset used to initialise the eigenbasis.

are shown in the central column of Figure 1. As well as the eigenspectra being visibly less noisy, the PCA now identifies more physical features, linking together in a single eigenspectra those features we know to be correlated, e.g., the Balmer Hydrogen line series in the second eigenspectrum, and emission lines in the third eigenspectrum. The left hand panel of Figure 2 shows the convergence with iteration number of the top six eigenvalues, which represent the variance in the dataset described by each corresponding eigenspectrum. The first eigenspectra converges quickly, after only a few iterations. The later eigenspectra converge more slowly.

While this iterative procedure results in a clean set of eigenspectra, the removal of outliers based on single components can easily lead to the loss of information from the dataset. This occurs when more unusual spectra, which would appear in later eigenspectra, are thrown out as outliers in the top few components. Additionally, running a full PCA for multiple iterations is undeniably an inefficient use of computing power, especially for large samples like the SDSS, where a single iteration takes about 2 days. We will now describe the application of the iterative and robust PCA algorithm to the same noisy dataset, showing that the same noise free and physically interesting eigenspectra are recovered, more quickly and without the physical removal of spectra from the dataset.

3.2 Robust Eigenspectra

Next we apply the streaming PCA method introduced earlier. For the actual implementation, we utilise a Cauchy-type ρ -function:

$$\rho(t) = \frac{2}{\pi} \arctan\left(\frac{\pi t}{2 c^2}\right) \quad (23)$$

and use the scalar c to adjust the asymptotic value of the scale estimate to match the standard deviation of a Gaussian point process. First we perform a classic PCA on 200 randomly selected spectra to provide the initial eigenbasis, and the initial σ^2 estimate (eq.19) is calculated from the sum of the residuals between these 200 spectra and their PCA reconstructions. We set $\alpha = 1 - 1/N$ where N is the total number of galaxies in the dataset. We also set $\delta = 0.5$ to maximize the breakdown point, which yields $c \simeq 0.787$ for our choice of ρ -function. Our final results are robust to variations in the size and content of the initialisation dataset and the precise method

used to initialise σ . Changes to α and δ alter the speed of convergence and susceptibility to outliers as the algorithm proceeds in time. Starting from the 201st spectrum, we input the spectra into the robust streaming PCA algorithm. The right hand panel of Figure 2 shows the progression of the eigenvalues with spectrum number. We see that full convergence of the top three eigenspectra is reached in less than one round of the 3485 spectra; naturally eigenspectra which carry less of the sample variance converge more slowly as they depend on the higher eigenvalue components but still not take more than two rounds of iterations to stabilize.

The third column of Figure 1 shows the resulting mean and top four eigenspectra. In this test case, the eigenspectra are very similar to those from the trimmed PCA but minor improvements are apparent. It is worth noting that the PCA algorithm is completely independent of the order of the bins: it has no spatial coherence. Hence the fact that our eigenspectra are smoother than the trimmed basis is already an indication of them being more robust.

4 DISCUSSION

There are two important points that an effective spectral eigenbasis must obey: (1) the eigenspectra should not introduce noise into the decomposition of individual galaxy spectra by being noisy themselves; (2) the top few eigenspectra must primarily describe the variance in the majority of the dataset, and not be influenced by minority outliers. Additionally, the eigenbasis should be quick to calculate and without the need for excessive memory storage.

Figure 1 illustrates the success of robust statistics for addressing point (1). The second point becomes clear when we investigate the distribution of the principal component amplitudes of the 3485 VVDS spectra. In Figure 3 we present the first two principal component amplitudes for the VVDS spectra using each of the eigenbases. The overall correlation between these first two principal component amplitudes for the classic PCA indicates the failure of this eigenbasis to represent the variance in the majority of the galaxy spectra: the basis has been influenced by outliers.

A final, important aspect of the new algorithm is the increase in speed. The iterative truncation approach to classic PCA is clearly inefficient, although the precise increase in speed will vary depend-

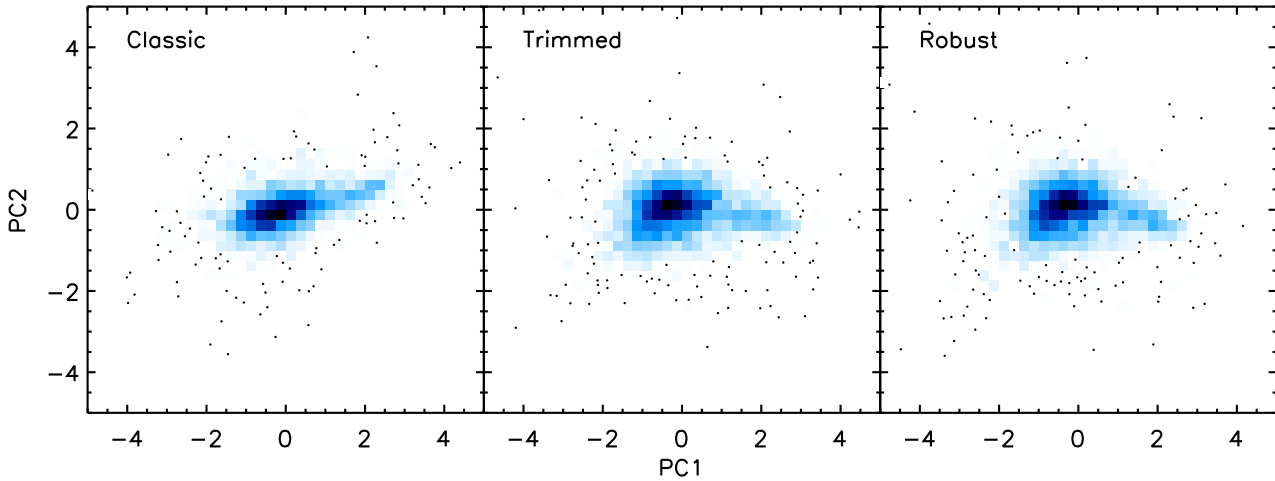


Figure 3. The joint distribution of the first two principal component amplitudes for the VVDS collection of 3485 spectra using the eigenbases presented in Figure 1. In order to focus on the main sample of objects, the axes are scaled such that outliers are not shown. From left to right: classic PCA using SVD, trimmed PCA with iterative removal of outliers, our robust PCA from the randomised streaming algorithm.

ing on dataset properties. For our VVDS test case the 20 iterations of classic PCA take five times longer than a single iteration of the 3485 spectra using the robust algorithm. The ratio will naturally change in favour of the new technique for larger collections of spectra.

5 SUMMARY

We present a novel method for performing PCA on real-life noisy and incomplete data. Our analysis is statistically robust, and implements the current state-of-the-art theoretical approach to generalising the classic analysis. Our streaming technique improves the eigensystem step-by-step when new observations are considered, and allows for direct monitoring of the improvement. The convergence is controlled by a single parameter that sets the effective sample size. The relevance of this parameter becomes obvious for very large datasets such as the SDSS catalog. These large samples are very much redundant in the statistical sense, i.e., often the analysis of a smaller subset yields as good results. Our method provides diagnostic tools to ensure convergence while enabling the selection of smaller effective sample sizes. The resulting eigenbasis has less noise than a classic PCA, and represents the variance in the majority of the data set without being influenced by outliers. Compared to a common work-around for reducing the effect of outliers on the eigenbasis by excluding extreme instances analogously to the trimmed mean calculation, the new algorithm provides a noticeable improvement in robustness and a substantial increase in speed. A production implementation within the NVO² Spectrum Services³ (Dobos & Budavári 2008) will be released where users of the site and Web services can direct the result sets of queries to the robust PCA engine. On this site we will publish the IDL scripts used for illustrations in this paper.

6 ACKNOWLEDGMENTS

The authors would like to thank the VVDS Team for making the spectra publicly available along with their metadata. Special thanks to Bianca Garilli for her help with obtaining the data. TB is grateful to Ricardo Maronna for his invaluable insights into robust statistics. The authors acknowledge useful discussions with Gerard Lemson and István Csabai. This work was supported by the Gordon and Betty Moore Foundation via GBMF 554 and the MAGPop European Research Training Network, MRTN-CT-2004-503929. AS was supported at MPA by the A. von Humboldt Foundation. TB at ELTE and LD were partially supported by MTA97-OTKA049957-NSF, NKTH:Polányi, RET14/2005, KCKHA005.

References

- Balogh M. L., Morris S. L., Yee H. K. C., Carlberg R. G., Ellingson E., 1999, *ApJ*, 527, 54
- Budavári, T., Szalay, A. S., Connolly, A. J., Csabai, I., Dickinson, M. E., 1999, *ASPC, Photometric Redshifts and the Detection of High Redshift Galaxies*, 191, 19
- Budavári, T., Szalay, A. S., Connolly, A. J., Csabai, I., & Dickinson, M. 2000, *AJ*, 120, 1588
- Connolly, A. J., Szalay, A. S., Bershad, M. A., Kinney, A. L., & Calzetti, D. 1995, *AJ*, 110, 1071
- Connolly, A. J., Csabai, I., Szalay, A. S., Koo, D. C., Kron, R. G., & Munn, J. A. 1995, *AJ*, 110, 2655
- Connolly, A. J., Budavári, T., Szalay, A. S., Csabai, I., & Brunner, R. J. 1999, *ASPC, Photometric Redshifts and the Detection of High Redshift Galaxies*, 191, 13
- Connolly, A. J., Szalay, A. S., Bershad, M. A., Kinney, A. L., & Calzetti, D. 1995, *AJ*, 110, 1071
- Connolly, A. J., & Szalay, A. S. 1999, *AJ*, 117, 2052
- Dobos, L., & Budavári, T., 2008, *ASP Conf. Ser., Vol. 382, The National Virtual Observatory: Tools and Techniques for Astronomical Research*, eds. M. J. Graham, M. J. Fitzpatrick, & T. A. McGlynn (San Francisco: ASP), p.147
- Everson R., & Sirovich L., 1995, *J. Opt. Soc. Am. A.*, 12, 8

² Visit the US National Virtual Observatory site at <http://us-vo.org>

³ Visit the Spectrum Services at <http://www.voservices.net/spectrum>

- Francis, P. J., Hewett, P. C., Foltz, C. B., & Chaffee, F. H. 1992, ApJ, 398, 476
- Glazebrook K., Offer A. R., Deeley K., 1998, ApJ, 492, 98
- Huber, P. J. 1981, Robust Statistics, Wiley Series in Probability and Statistics
- Karhunen, H. 1947, Ann. Acad. Science Fenn, Ser. A.I. 37
- Le Fèvre, O., et al. 2005, A&A, 439, 845
- Li, Y., Xu, J., Morphet, L., & Jacobs, R. 2003, Proceedings of IEEE International Conference on Image Processing
- Loève, M. 1948, Processus Stochastiques et Mouvement Brownien, Hermann, Paris, France
- Maronna, R. A. 2005, Technometrics, 47, 3
- Maronna, R. A., Martin, R. D., & Yohai, V. J. 2006, Robust Statistics: Theory and Methods, Wiley Series in Probability and Statistics
- McCracken H. J., Radovich M., Bertin E., Mellier Y., Dantel-Fort M., Le Fèvre O., Cuillandre J. C., Gwyn S., Foucaud S., Zamorani G., 2003, A&A, 410, 17
- Wild V., Hewett P. C. 2005, MNRAS, 358, 1083
- Wild V., Kauffmann G., Heckman T., Charlot S., Lemson G., Brinchmann J., Reichard T., Pasquali A. 2007, MNRAS, 381, 543
- Yip C. W., et al., 2004a, AJ, 128, 585
- Yip C. W., et al., 2004b, AJ, 128, 2603